Performance Optimization of Interference-Limited Multihop Networks

Ahmed Bader and Eylem Ekici, *Member, IEEE*

Abstract—The performance of a multihop wireless network is typically affected by the interference caused by transmissions in the same network. In a statistical fading environment, the interference effects become harder to predict. Information sources in a multihop wireless network can improve throughput and delay performance of data streams by implementing interference-aware packet injection mechanisms. Forcing packets to wait at the head of queues and coordinating packet injections among different sources enable effective control of copacket interference. In this paper, throughput and delay performance in interference-limited multihop networks is analyzed. Using nonlinear probabilistic hopping models, waiting times which jointly optimize throughput and delay performances are derived. Optimal coordinated injection strategies are also investigated as functions of the number of information sources and their separations. The resulting analysis demonstrates the interaction of performance constraints and achievable capacity in a wireless multihop network.

Index Terms—Hopping dynamics, interference-limited, multihop networks, performance optimization, Rayleigh fading.

I. INTRODUCTION

IN MULTIHOP wireless networks where all transmitters share the same radio channel, a packet propagating through the network suffers from harmful interference generated by peer packets in the network. The wireless link quality is determined by interference, which in turn determines the longest distance a packet can correctly be received at. As the level of mutual interference increases, packets experience shorter hopping distances and slower propagation speeds across the network. Therefore, the network performance is a function of the internally-generated interference. In this work, we aim to analyze the performance of an interference-limited multihop wireless network in terms of information transfer from sources to sinks. The following two performance metrics are considered for this purpose:

1) *Throughput (THR)*: The rate at which packets cross a measurement boundary that cuts each flow only once.
2) *Head-of-Queue Delay (HQD)*: The sum of the time a packet spends at the head of the source queue and the multihop transmission time towards its destination.

These two metrics are closely related to the transport rate metric which is the product of the throughput and the distance travelled by packets over a single hop [1]. However, transport rate on its own does not capture the end-to-end packet delivery latency as will be shown in Section V-C. This observation motivates our choice to introduce HQD as an additional and necessary performance metric. Given a finite set of source-sink pairs, we are interested in distinct packet flows traversing the network and not necessarily how many packets may coexist in the network.

The interference a packet suffers from can be classified as *intra-flow* and *inter-flow*. Interference from packets injected from the same source is referred to as intra-flow interference, whereas interference from packets belonging to other flows is referred to as inter-flow interference. The interdependence of THR and HQD in such networks leads to important observations. An increased packet injection rate of information sources (THR) leads to increased numbers of packets propagating in the network, which increases the mutual interference levels. Consequently, the progress of packets is slowed down and HQD is adversely affected. Hence, there is an inherent tradeoff between the achievable THR and HQD. This tradeoff can be controlled by managing packet injection processes at the sources, which constitutes the main objective of this study. Information sources can achieve desired tradeoff levels by introducing appropriate waiting times between injection of packets. Forcing packets to wait at the head of the source queue creates a controlled interference environment for the leading packets in the same flow. Moreover, information sources must coordinate their injection processes such that the adverse effects of inter-flow interference are minimized.

The analysis presented in this paper is performed for networks with unlimited node density. We are interested in understanding the statistical packet flow characteristics which optimize the network performance. For this purpose, we first introduce nonlinear models describing 1-D and 2-D packet flow dynamics under a probabilistic communication model. We then jointly consider THR and HQD in a multi-objective optimization problem, where we use nonlinear recursive methods to derive the optimal waiting times. We then devise local search techniques to derive the optimal number of flows and the optimal coordination for multiple-flow packet injection. Obtained results show the interactions between THR and HQD and achievable performance levels with respect to one metric when the other is used as a constraint.

II. RELATED WORK

In the literature, limitations of interference on the performance of multihop networks have been analyzed in a number of studies. In [1] and [2], asymptotic bounds on the achievable throughput and transport capacities under a deterministic

interference model are presented. It is shown that the achievable transport capacity per node vanishes as the number of nodes approaches infinity. The authors in [3] utilize a generalized fading channel model integrated with the use of channel state information (CSI). In [4], the achievable aggregate and per node throughput for three different classes of ad hoc multihop networks is studied. Routing-oriented capacity limits are also presented in [5].

Limitations imposed by internal interference on performance is also discussed in the literature in terms of packet reception probability. In [6], a probabilistic model for successful packet reception is developed. Based on a path-loss exponent model and Poisson node deployment, the authors investigate the problem of finding optimum transmission ranges. The limitations of using a deterministic radio propagation model are addressed in [7]. A generalized mathematical model is developed which describes the probability of successful packet reception under Rayleigh fading.

Graph-theoretical approaches are also available in literature. In [8], interfering links are modeled using a *conflict graph* to estimate the throughput of the network. An undirected geometric random graph is presented in [9] to analyze the connectivity of a multihop ad hoc network under lognormal shadowing. In [10], effects of interference on performance are studied for collision-based multihop networks. In [11], strategies and algorithms to construct optimum interference graphs in a TDMA-based network are presented.

In this study, we treat achievable performance from a macro perspective: We perceive packet flows as directional quantities and aim to deliver packets to their respective destinations while achieving desired performance levels. Therefore, the objective of the analysis presented in this paper is distinguishable from that of [1], which derives throughput and transport capacity bounds as functions of the number of nodes. In order to encompass the latency in communicating information between sources and destinations, we introduce the HQD metric. In this study, THR and the HQD are jointly considered as criteria for deriving optimal packet injection mechanisms.

The link model presented in [7] is utilized as the basic tool for our analysis. We show that this model is valid for different time-selectivity scales of the fading channel. Thus, two interpretations are given for the model in terms of link outage and link reliability criteria. We also provide an equivalent upperbound representation of the model that is useful when there is no knowledge about the locations of interferers. We introduce nonlinear models describing 1-D and 2-D packet hopping dynamics under the developed communication model. Moreover, we present simple optimization techniques that are specifically tailored to optimize this highly nonlinear problem.

III. COMMUNICATION MODEL

A. Channel Model

In this study, a narrowband multipath wireless channel with a coherence time longer than bit transmission time is assumed. This channel is modeled as a multiplicative frequency nonselective Rayleigh fading channel with a large-scale path-loss
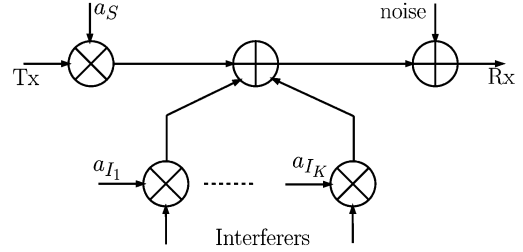

Fig. 1. Block diagram of the channel model.

exponent α [12]. An omnidirectional antenna pattern is assumed for all nodes, which emits at the same power P. For a certain packet transmission, the desired signal at the receiver is corrupted by K interference signals and a zero-mean additive white Gaussian noise (AWGN) signal z of variance N as shown in Fig. 1. Each transmitted signal goes over an independent Rayleigh fading channel. a_S and $\{a_{I_k}\}_{k=1}^{K}$ are independent random fading coefficients with Rayleigh-distributed magnitudes and uniform phases. The desired signal strength is denoted by S and the signal strength of the kth interferer by $I_k, k = 1, 2, \ldots, K$. Furthermore, the distance between the transmitter and the receiving node is denoted by d_S. The distance between the kth interferer and the receiver is denoted by d_{I_k}, where $k = 1, 2, \ldots, K$. The mean power content in the channel over which the desired signal is transmitted equals the large-scale path loss, i.e., $\mathbb{E}[|a_0|^2] = (\frac{\lambda}{4\pi})^{\alpha} d_S^{-\alpha}$, where λ is the wavelength. Similarly, the mean power content in the kth interferer's channel is given by $\mathbb{E}[|a_k|^2] = (\frac{\lambda}{4\pi})^{\alpha} d_{I_k}^{-\alpha}$. Under the Rayleigh fading channel model, S and I_k are exponentially distributed with means $\bar{S} = \mathbb{E}[|a_0 v_0|^2] = P_0 d_S^{-\alpha}$ and $\bar{I}_k = \mathbb{E}[|a_k v_k|^2] = P_0 d_{I_k}^{-\alpha}$, respectively, where $P_0 \triangleq P(\frac{\lambda}{4\pi})^{\alpha}$. The signal-to-interference-and-noise ratio (SINR), denoted by γ, is given by

$$\gamma = \frac{S}{N + \sum_{k=1}^{K} I_k}. \tag{1}$$

Furthermore, we denote the ratio between the mean desired signal and the noise power by γ_0 and the ratio of the mean desired signal power to the mean interference power from the kth interferer by η_k, where

$$\gamma_0 = \frac{\bar{S}}{N} = \frac{P_0 d_S^{-\alpha}}{N}, \quad \eta_k = \frac{\bar{S}}{\bar{I}_k} = \left(\frac{d_S}{d_{I_k}}\right)^{-\alpha}. \tag{2}$$

The cumulative density function (cdf) $F(\gamma)$ of the SINR is [7]

$$F(\gamma) = 1 - e^{-\frac{\gamma}{\gamma_0}} \prod_{k=1}^{K} \frac{1}{1 + \frac{\gamma}{\eta_k}}. \tag{3}$$

B. Link Model

The quality of the wireless link may be tracked by observing the instantaneous bit error rate (BER). However, the analysis involving the BER must assume a certain modulation class and usually involves complicated mathematical functions. A more general way to capture the quality of a wireless link is through its outage probability, which is defined as *the probability that the*

instantaneous SINR (γ) *falls below a certain specified threshold* γ_t [13].

The effects of multiplicative fading on the SINR may be projected on two different time scales: the bit duration and the packet transmission time. In case the coherence time is greater than the packet transmission time, the probability of outage is time-invariant for a given packet transmission. A packet is successfully received if $\gamma \geq \gamma_t$. Using (3), the probability of correct packet reception is given as

$$\mathbb{P}[\gamma \geq \gamma_t] = 1 - F(\gamma_t) = e^{-\frac{\gamma_t}{\gamma_0}} \prod_{k=1}^{K} \frac{1}{1 + \frac{\gamma_t}{\eta_k}}. \quad (4)$$

This case is also referred to as a quasi-static or block fading channel. A common design strategy is to condition the wireless link against a desired minimum reliability [14]–[16]. For a desired link reliability of $1 - \tau$ where $0 < \tau < 1$, the link condition is expressed as $\mathbb{P}[\gamma \leq \gamma_t] \leq \tau$.

We also consider the more general case where the fading channel is only slow with respect to the bit duration but not to the packet transmission time, i.e., the coherence time is much less than the packet duration. In this case, the probability of incorrect bit reception is $\mathbb{P}[\gamma \leq \gamma_t]$. The conditions for successful packet reception are highly dependent on the decoding scheme. This often requires determining the frequency of occurrence and the average duration of deep fades during the transmission of one packet. This can be obtained by performing a threshold-crossing analysis [17], [18]. However, for the the sake of simplicity, we assume that the fading process is fast enough to produce approximately uncorrelated channel gains every time a bit is transmitted. Uncorrelated bit decisions can also be achieved using proper bit interleaving. Moreover, we assume that a packet is successfully decoded if the number of incorrect bits is less than a certain fraction τ, which can be viewed as a measure of tolerance to link outage. Given the average ratio of incorrect bits to the total packet length $\mathbb{P}[\gamma \leq \gamma_t]$, the condition for successful packet reception can be written as

$$\mathbb{P}[\gamma \leq \gamma_t] \leq \tau$$
$$e^{-\gamma_t/\gamma_0} \prod_{k=1}^{K} \frac{1}{\left(1 + \frac{\gamma_t}{\eta_k}\right)} \geq 1 - \tau \quad (5)$$

which is the same link condition specified for the case of a block fading channel. Within this context, the block fading channel is a special case of the general time-selective fading model. In the subsequent analysis, we will assume a general time-selective fading model.

Since the fading coefficients are assumed to be independently distributed (Section III-A), the events of successful packet reception at locations that are sufficiently apart are independent. It follows that the events of successfully receiving a packet every time it hops are also independent. Furthermore, we note that the link condition is specified in this manner to avoid retransmissions, i.e., first-time delivery is sought. It is also important to note that the choice of γ_t and τ is affected by the hardware, modulation, and error-correction schemes [19] which may largely vary from one application to another. Consistent with [15, Theorem 1], the left-hand side of the link condition in (5) can be

factorized into two parts: the contribution of the noise and that of the interference. Furthermore, the contribution of each interferer can be explicitly identified from the link condition.

The link condition in (5) may also be expressed in terms of the packet transmission distance d_S and the interference distances $\{d_{I_k}\}_{i=1}^{K}$. Incorporating (2) into (5) yields

$$\beta d_S{}^\alpha + \sum_{k=1}^{K} \ln\left(1 + \gamma_t \left(\frac{d_S}{d_{I_k}}\right)^\alpha\right) \leq \ln\left(\frac{1}{1 - \tau}\right) \quad (6)$$

where $\beta = \frac{N\gamma_t}{P_0}$. For a given network setting, we are interested in finding the maximum distance d_S a packet can hop and the corresponding values of $\{d_{I_k}\}_{k=1}^{K}$ such that the link condition is *just* satisfied. On the other hand, in the absence of interference $(\eta_k = \infty, \forall k)$, the link condition reduces to $e^{-\beta d_S{}^\alpha} \geq 1 - \tau$. The packet hop distance in this case is denoted by d_0 and is upper bounded by $\sqrt[\alpha]{\frac{-1}{\beta} \ln(1 - \tau)}$.

C. Monotonicity of the Hopping Distance

It can be shown that the hopping distance of a packet is an increasing monotone in the summation of the interference distances $\sum_k d_{I_k}$. From (6), it is apparent that d_S is monotonically increasing in any of the interference distances $\{d_{I_k}\}_{k=1}^{K}$. Since $d_{I_k} > 0, \forall k$, then this implies that d_S is also monotonically increasing in $\sum_k d_{I_k}$. This result, although simple, is important and will be used in subsequent discussions.

D. Bounded Representation of the Link Condition

In the absence of information about the relative locations of the packet transmitters, it is still possible to calculate the hop distances. Using $(d_S/d_{I_k})^{-\alpha} = \bar{S}/\bar{I}_k$ in (6), we obtain

$$\beta d_S{}^\alpha + \sum_{k=1}^{K} \ln\left(1 + \gamma_t \frac{\bar{I}_k}{\bar{S}}\right) \leq \ln \frac{1}{1 - \tau}. \quad (7)$$

For small values of τ, $\ln(1 + \gamma_t \bar{I}_k / \bar{S})$ is approximated by the first three terms of its McLaurin series

$$\ln\left(1 + \gamma_t \frac{\bar{I}_k}{\bar{S}}\right) \approx \frac{\gamma_t}{\bar{S}} \bar{I}_k - \frac{1}{2} \left(\frac{\gamma_t}{\bar{S}}\right)^2 \bar{I}_k^2 + \frac{1}{3} \left(\frac{\gamma_t}{\bar{S}}\right)^3 \bar{I}_k^3. \quad (8)$$

If the summation of the average interference powers (denoted by A_1) is known, the probability of reception may be simplified in terms of its upper bound. We denote the second- and third-order summation of the average interference powers by A_2 and A_3, respectively, such that we have $A_1 = \sum_{k=1}^{K} \bar{I}_k, A_2 = \sum_{k=1}^{K} \bar{I}_k^2$ and $A_3 = \sum_{k=1}^{K} \bar{I}_k^3$. Since all summations run over positive terms, we have $A_2 < A_1^2$ and $A_3 < A_1^3$. Furthermore, using Jensen's inequality, we get $A_2 \geq A_1^2/K$. Using these relationships, and under the reasonable assumption that $0 < \bar{I}_k \ll 1$, the link condition is expressed as

$$\beta d_S{}^\alpha + \left(\frac{\gamma_t}{\bar{S}}\right) A_1 - \frac{1}{2} \left(\frac{\gamma_t}{\bar{S}}\right)^2 \frac{A_1^2}{K}$$
$$+ \frac{1}{3} \left(\frac{\gamma_t}{\bar{S}}\right)^3 A_1^3 \leq \ln\left(\frac{1}{1 - \tau}\right). \quad (9)$$

From (9), we obtain a lower bound on the achievable hop distance of a certain packet given that the averages of the interfer-
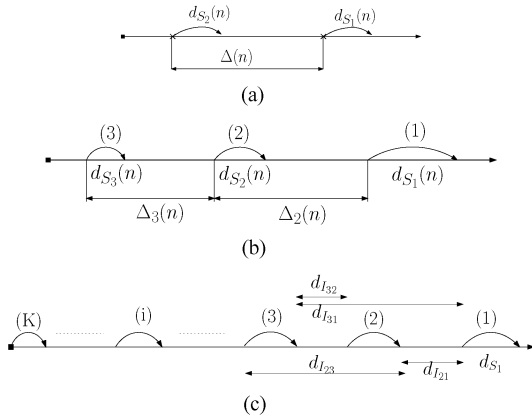
Fig. 2. Hopping along a linear network. (a) Network with two packets. (b) Network with three packets. (c) Network with K packets.
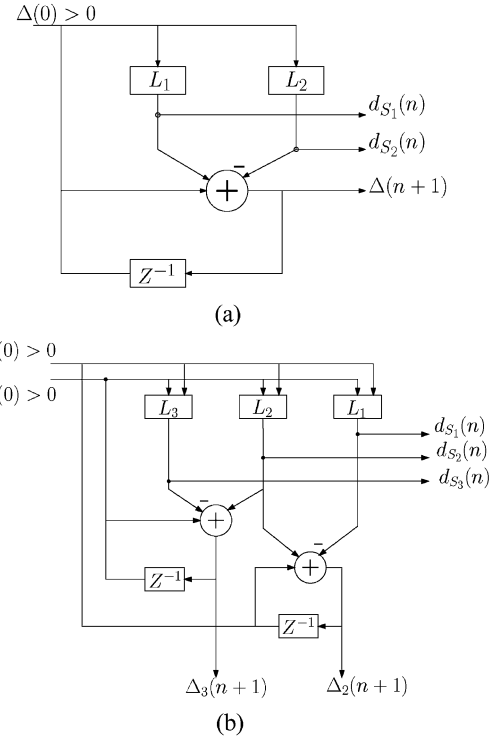

Fig. 3. IIR hopping system representation. (a) IIR representation of a two-packet hopping system. (b) IIR representation of a three-packet hopping system.

ence signals are available. Knowledge of the locations of peer packets is not required in this case.

IV. PACKET-HOPPING DYNAMICS IN A LINEAR NETWORK

Here, the hopping behavior of packets under the communication model described in Section III is investigated. We study first a linear network as a stepping stone towards developing hopping models for the 2-D case.

A. Assumptions

The following assumptions are made for the analysis of packet-hopping dynamics.

1) *Integer time scale*: Synchronous transmissions of fixed-length packets are assumed. Hence, time is represented with integer values.
2) *Unlimited node density*: Packets are delivered to the farthest point possible towards their destination.
3) *Packet uniqueness*: There are no duplicates of the same packet in the network. Gains of cooperative relaying strategies [20] are acknowledged. However, we are interested in studying the effect of interference on the number of distinct packets a multihop network may handle.
4) *Infinite source queue length*: We assume that all packets are available at the source at injection time.
5) *Packet hop distances*: Packets hop the maximum distance possible under the link condition in (6).
6) *Path-Loss Coefficient α*: Without loss of generality, a path-loss coefficient of $\alpha = 2$ is assumed.

We note that the unlimited node density assumption may serve as a good direct approximation of dense networks such as dense sensor networks. However, as we will show in subsequent sections, the optimal operation of the network can be sustained with finite node densities. Furthermore, this approach also allows us to concentrate on the achievable capacity of a multihop wireless network subject to other performance constraints. Finally, we assume that the intermediate nodes do not buffer packets and relay to the next hops as soon as they are received. This allows us to control the packet scheduling through the scheduling at source nodes alone.

B. IIR Modeling of Hopping Dynamics

The hopping dynamics of packets in a linear network are best modeled by an infinite impulse response (IIR) system. We next consider simple cases which justify this choice.

1) Two-Packet Hopping System: Fig. 2(a) shows a two-packet linear network where the transmitters are separated by a distance Δ. The packet numbering plan follows the order of the packets at the source queue. Time is denoted by n. The hopping distance of the first packet at time n is $d_{S_1}(n)$ and that of the second packet is $d_{S_2}(n)$. At $n = 0$, the packets are separated by $\Delta(0)$. Packets will be able to start hopping only if $\Delta(0) > 0$. The system is governed by the following link conditions:

$$L_i : e^{-\beta d_{S_i}{}^2(n)} \left/ \left[1 + \frac{\gamma_t}{\left(\frac{\Delta(n)}{d_{S_i}(n)} + (-1)^{i-1} \right)^2} \right] \ge 1 - \tau \right.$$

$$(10)$$

where $n = 0, 1, 2, \cdots$ and $i = 1, 2$. Given $\Delta(n)$, packet hop distances are found by solving for $d_{S_i}(n)$, which just satisfies the link condition in (10). Every time the packets hop, the next inter-packet separation distance is found using the update equation $\Delta(n+1) = \Delta(n) + d_{S_1}(n) - d_{S_2}(n)$. Therefore, it is very convenient to describe the hopping behavior of the network with an IIR system, which is initially excited by $\Delta(0)$. The representation of a two-packet IIR system is shown in Fig. 3(a). It is assumed that $\Delta(-1) = 0$ such that $d_{S_1}(0) = d_{S_2}(0) = 0$.

2) Three-Packet Hopping System: The network in Fig. 2(b) is initially excited by $\Delta_2(0)$ and $\Delta_3(0)$. We assume that $\Delta_2(-1) = \Delta_3(-1) = 0$ such that $d_{S_1}(0) = d_{S_2}(0) =$

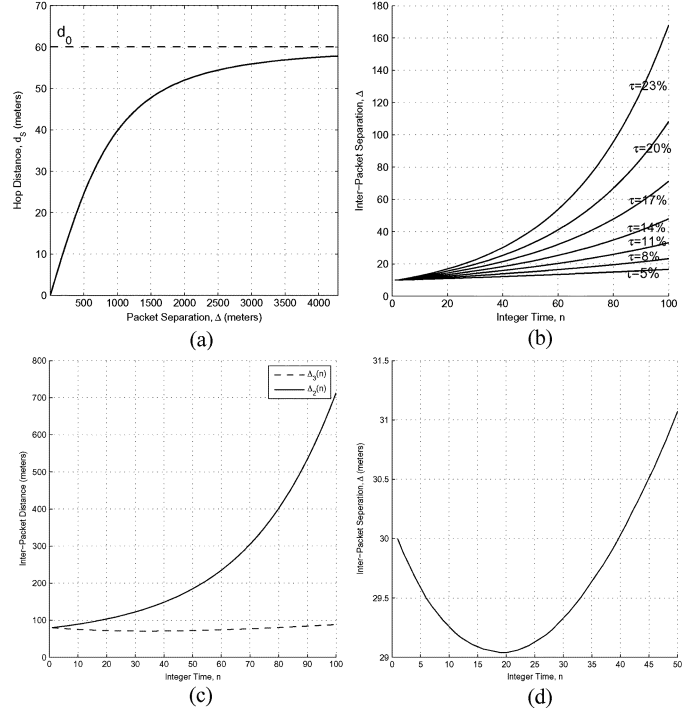| Parameter	Description	Value
P	transmit power	10 dBm
N	noise level	-80 dBm
τ	tolerance to link outage/ tolerance to link non-availability	5%
γ_t	SINR outage threshold	10 dB
λ	wavelength	1/3 m

Fig. 4. Properties of two- and three-packet hopping systems. (a) Hop distance versus inter-packet separation (two-packet system). (b) Inter-Packet separation versus time (two-packet system). (c) Packet decoupling property: inter-packet separations versus time (three-packet system). (d) Self-adjusting property (three-packet system).

$d_{S_3}(0) = 0$. The update equations for this system are: $\Delta_i(n+1) = \Delta_i(n) + d_{S_{i-1}}(n) - d_{S_i}(n), i = 1, 2$. The link conditions L_1, L_2 and L_3 are given by

$$e^{-\beta d_{S_i}(n)} \Big/ \prod_{j=1, j\neq i}^{3} \left[1 + \frac{\gamma_t}{\left(d_{I_{i,j}}(n)/d_{S_i}(n)\right)^2} \right] > 1 - \tau \tag{11}$$

where $d_{I_{i,j}}(n)$ is the distance from the jth interferer to the receiver of the ith packet. The corresponding IIR system representation is shown in Fig. 3(b). As the order of the IIR system increases, it is only possible to find the hop distances numerically. The hop distance of the ith packet is found by gradually increasing $d_{S_i}(n)$ in (11) until the link condition is just met. Higher order hopping system models are built in a similar manner. However, we utilize at most the three-packet hopping system as it suffices for the analysis.

C. Fundamental Properties

Here, we present some properties of the hopping behavior of packets along a linear network. These properties are used by information sources when deriving the optimal packet injection mechanisms (Sections V and VI). Numerical results in the rest of the analysis are obtained using the values in Table I.

1) Upper Bound on the Packet Hop Distance: From (10), the inter-packet distance Δ at time n may be expressed explicitly in terms of the hop distance d_{S_i}, which has a positive first derivative, i.e., Δ is monotone in d_S, and hence the converse is true. Moreover, taking the limit $\Delta \to \infty$ in the link condition of (10) gives the interference-free hop distance: $\lim_{\Delta \to \infty} d_{S_i} = \sqrt{\frac{-1}{\beta} \ln(1 - \tau)} = d_0$. As a result, the hop distance is concave and upper-bounded in terms of the inter-packet separation as shown in Fig. 4(a).

2) Increasing Gap: The network settings in Fig. 2 show that the receiver of the leading packet (first packet) always suffers from the least interference. Thus, the hopping distance of the first packet d_{S_1} is always larger than those of the other packets. Therefore, the gap between the leading packet and the trailing packets widens with time. For instance, in the two-packet system this corresponds to $\lim_{n\to\infty} \Delta = \infty, \lim_{n\to\infty} d_{S_i} = d_0$. It will be shown next that this property applies to linear network with an arbitrary number of packets, i.e., the gap between any two successive packets widens with time. This can formally be demonstrated by considering Fig. 2(c). The interference distance from the jth packet to the ith packet is denoted by $d_{I_{ij}}$, i.e., the distance between the receiver of the ith packet and the transmitter of the jth packet. The proof of this property follows two steps.

Step 1) Show that the gap between the first and second packets grows with time.

Step 2) Extend the result to subsequent packets in the linear network.

Step 1: With reference to Fig. 2(c), $d_{I_{12}} > d_{I_{21}}$ and $d_{I_{1k}} > d_{I_{2k}}, \forall k = 3, \ldots, K$. Using the monotonicity result of Section III-C, $\frac{\partial d_{S_i}}{\partial \sum_j d_{I_{ij}}} > 0$ must hold. Since $\sum_j d_{I_{1j}} > \sum_j d_{I_{2j}}, d_{S_1}(n) > d_{S_2}(n)$ must hold $\forall n$. As $\Delta_2(n+1) = \Delta_2(n) + d_{S_1}(n) - d_{S_2}(n), \Delta_2(n+1) > \Delta_2(n)$ holds $\forall n$.

This shows that the gap between the first and second packets grows with time. This is also true for the gap between subsequent successive packets, although the gap may initially shorten for a limited period of time. Step 2 of the proof demonstrates this. Consider Fig. 2(c) for the second step.

Step 2: Using the monotonicity property of Section III-C, $d_{S_3} > d_{S_2}$ iff $d_{I_{21}} + d_{I_{23}} < d_{I_{31}} + d_{I_{32}}$. These terms can be rearranged to obtain $\Delta_2 - d_{S_2} + \Delta_3 + d_{S_2} < \Delta_2 + d_{I_{32}}$. From this, we also obtain $\Delta_3 < 2(\Delta_3 - d_{S_3})$, and therefore $\Delta_3 > 2d_{S_3}$. As long as $\Delta_3 > 2d_{S_3}, d_{S_3}(n+1) > d_{S_3}(n)$ and $d_{S_2}(n+1) < d_{S_2}(n)$ implies $\Delta_3(n+1) < \Delta_3(n)$. However, $d_{S_1}(n+1) > d_{S_1}(n), \forall n$, also implies $\exists n'$ such that $d_{I_{21}}(n') + d_{I_{23}}(n') > d_{I_{31}}(n') + d_{I_{32}}(n')$. Therefore, we conclude that $\Delta_3(n'+1) > \Delta_3(n'), n > n'$.

This shows that the gap between the second and third packets may initially reduce but will regain its growing behavior. This is what we refer to as the *"self-adjusting property"*. Fig. 4(d) illustrates this property by tracking the inter-packet separation

$\Delta_3(n)$ with time. The same two-step proof can also be applied to show the increasing gap property for all packets.

3) Time Evolution of the Inter-Packet Separation: The increasing gap property takes longer periods to observe for small values of link outage tolerance τ. To demonstrate this, we plot the inter-packet separation $\Delta(n)$ in a two-packet system versus time for various values of τ. The larger τ is, the more relaxed the link condition becomes. Therefore, the growth in the inter-packet separation over time is slower for smaller τ, as shown in Fig. 4(b). For more reliable communication, it is desirable to have τ as small as possible, even in noisy environments. Under such circumstances, it may be assumed that the inter-packet separation stays constant in the vicinity of the source. This corresponds to the lowest curve ($\tau = 0.05$) in Fig. 4(b). In other words, both packets cover almost equal hop distances. The situation where τ is required to be small in the existence of high noise level will be referred to as *"strict network conditions."* It can be also shown that the hop distances of both packets increase very slowly under strict network conditions, and they appear to hop at the same constant speed.

4) Packet Decoupling Property: The constant inter-packet separation between two packets under strict network conditions holds only until a third packet is injected. Injecting a third packet will impose more interference on the second packet than the first, and therefore it will "decelerate" the second packet such that the first packet will be able to "break free" from the group. This is illustrated in Fig. 4(c). Similarly, when a fourth packet is injected into the network, it will have a decelerating effect on the third packet such that the second packet will be able to speed up its pace. Consequently, a packet i ready to be injected at the head of the source queue will suffer from interference mainly from the two packets ahead, i.e., the $(i-1)$st and $(i-2)$nd packets. This property is utilized to study the optimization of the packet injection process.

V. OPTIMAL PACKET INJECTION IN LINEAR NETWORKS

Here, we first show that maximizing throughput on its own saturates the network and deteriorates the HQD performance. Then, we propose to optimize the packet injection mechanism by jointly considering HQD and THR. Using the linear hopping properties presented in Section IV-C, we calculate optimal waiting times, which are shown to converge.

A. THR and HQD in Linear Networks

Throughput at any point along the network is defined as the rate at which packets cross a measurement boundary. If the boundary is chosen at the information source, then the measured rate represents the source throughput, THR. The definition of throughput implies that it is a time-varying quantity which is sensitive to the location of the measurement boundary. We will show here that moving the measurement boundary along an infinitely-long linear network produces a throughput which asymptotically converges to zero. This claim can be verified by utilizing the asymptotic results given in Section IV-C2. We consider a packet j which is hopping along an infinitely-long linear network parallel to the positive x-axis. Its hop distance at time n at distance x from the source is denoted by $d_{S_j}(x,n)$. Similarly, its separation from the leading packet $(j-1)$ is denoted
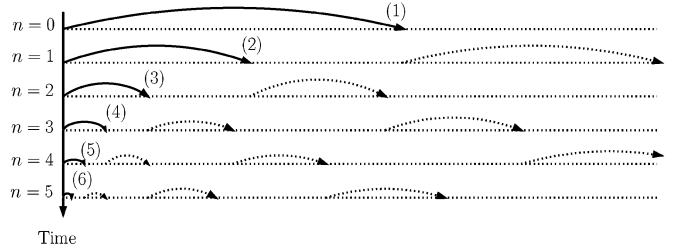

Fig. 5. Diminishing first hop distance for a unit inter-packet waiting time.

by $\Delta_j(x,n)$. As the packet progresses along the network, the following limits hold true:

$$\lim_{x\to\infty,n\to\infty} \Delta_j(x,n) = \infty \tag{12}$$

$$\lim_{x\to\infty,n\to\infty} d_{S_j}(x,n) = d_0. \tag{13}$$

This indicates that it takes a longer time to observe two subsequent packets crossing an observation point as the observation point is moved along the x-axis. As a result, throughput is a decreasing function of the distance from the source. Furthermore, it follows from (13) that throughput asymptotically falls to zero as a function of x. This result does not contradict with the principle of flow conservation since none of the packets is buffered or lost at the intermediate forwarding nodes. It is only that packets stretch apart from each other as they progress towards the destination. In practice, network lengths are limited. Under strict network conditions where the time evolution of the network dynamics is slow, it is very difficult to observe such a result.

In most cases, it is desirable to maximize the source throughput (THR). This corresponds to minimizing the inter-packet waiting time. Based on the assumption of unlimited node density in Section IV-A, injecting a packet every time unit becomes feasible. With unlimited density, packets may hop arbitrarily small distances as long as the link conditions for all packets are satisfied. Therefore, there are no restrictions on injecting a packet every unit time. In this case, the maximum bit-throughput is just equal to the wireless link bandwidth. However, whenever a new packet is injected from the source queue, its first hop inside the network will be shorter than the first hop of the preceding packet, as illustrated in Fig. 5. This is intuitive and can be verified as follows.

1) From (5), it can be shown that for any packet i just injected from the source queue, the following strict lower bound on η_{i-1} must be attained for successful packet reception:

$$\eta_{i-1} = \frac{\bar{S}_i}{\bar{I}_{i-1}} = \left(\frac{d_{I_{i-1}}}{d_{S_i}}\right)^\alpha > \gamma_t\left(\frac{1}{\tau}-1\right). \tag{14}$$

It follows from (14) that $d_{S_i} < d_{I_{i-1}} \Rightarrow d_{S_i} < \Delta_i$, i.e., the initial hop distance of a packet is always less than the separation from the next leading packet.

2) Since packets are injected at rate-1, it follows that at time n and with $i \geq 1$, we have $\Delta_i = d_{S_{i-1}}$, where $d_{S_{i-1}}$ is the initial hop distance of the $(i-1)$st packet made at time $n-1$.

$d_{S_i}^{(j)}$	The distance the ith packet hops just after the jth packet is injected, where $i \leq j$.
$\Delta_i^{(j)}$	the distance between the transmitters of the ith and $(i-1)$th packets just after the jth packet is injected.
n_i	The waiting time of the ith packet at the source queue.

3) Consequently, $d_{S_i} < d_{S_{i-1}}$, where the inequality is strict. Therefore, we obtain the following limit:

$$\lim_{i \to \infty} d_{S_i} = 0. \tag{15}$$

As the source queue is drained out, the initial hop distance of an injected packet diminishes. As a result, source throughput on its own does not constitute a useful performance criterion since it is indifferent to the packet delivery delay requirements. Injecting packets at rate-1 results in a progress which asymptotically falls to zero as $n \to \infty$. At the other extreme, waiting too long may allow the packet at the head of the queue to hop at the noise-only upper bound d_0. However, this can only be achieved if all preceding packets reach the destination node, which can incur very high delays. Therefore, the goal is to find optimal waiting times to achieve a tradeoff between HQD and THR. We first find optimal waiting times by only considering the HQD criterion. The analysis in this case is shown to be readily usable to jointly consider both criteria.

B. Minimization of HQD in Strictly Conditioned Linear Networks

As discussed in Section IV-C3, under strict network conditions, hop distances of packets in the vicinity of the source are almost equal and grow by insignificant amounts with time. The injection of packets are considered in a recursive manner starting from the first packet. For each packet, the waiting time which minimizes the HQD is computed. The injection of one packet provides the necessary information for the calculation of the optimal waiting time for the next packet in the source queue. Packets are numbered according to their order in the source queue. The notation is detailed in Table II.

1) First and Second Packets: The first packet is injected in an interference-free environment. Therefore, its initial hop distance is d_0. The injection of the second packet inevitably slows down the first packet. After the second packet is injected, both packets take approximately equal-length hops. Hence, the inter-packet separation is given by $n_2 d_0$, where n_2 is the waiting time of the second packet. The link condition for the second packet at the instant it is injected is expressed as

$$\beta d_{S_2}^{(2)2} + \ln\left[1 + \gamma_t \left/ \left(\frac{n_2 d_0}{d_{S_2}^{(2)}} - 1\right)^2\right.\right] \leq \ln\left(\frac{1}{1-\tau}\right). \tag{16}$$

The HQD T_2 for the second packet is given as $T_2 = l/d_{S_2}^{(2)} + n_2$, where l is the length of the network. The relationship between
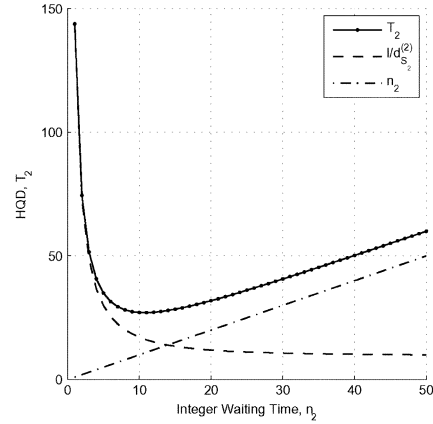

Fig. 6. Convexity of HQD in terms of waiting time of the second packet.

$d_{S_2}^{(2)}$ and n_2 under (16) may be approximated with great accuracy as

$$d_{S_2}^{(2)} = d_0(1 - e^{-n_2/\alpha_2}) \tag{17}$$

where α_2 is a fitting coefficient that is network-dependent. From (17), waiting too long, $(n_2 \to \infty)$ yields an interference-free hop distance. The HQD function can be expressed in terms of n_2 as

$$T_2 = \frac{l}{d_0(1 - e^{-n_2/\alpha_2})} + n_2. \tag{18}$$

Since the second derivative $\frac{d^2 T_2}{dn_2^2} > 0$, T_2 is convex in n_2 as shown in Fig. 6. Therefore, there exists an optimal waiting time $n_{2_{\text{opt}}}$ which minimizes T_2. Solving for n_2 in $\frac{dT_2}{dn_2} = 0$ yields the waiting time at which the T_2 curve is minimum as

$$\tilde{n}_2 = \alpha_2 \ln\left(\frac{2d_0\alpha_2}{l + 2d_0\alpha_2 - \sqrt{l^2 + 4ld_0\alpha_2}}\right). \tag{19}$$

Since time only assumes integer values, the actual optimal waiting time is the integer value at which the absolute value of the slope of the $T_2(n_2)$ curve is smallest. Therefore, the optimal waiting time $n_{2_{\text{opt}}}$ is calculated as

$$\left|\frac{dT_2}{dn_2}\Big|_{\lfloor\tilde{n}_2\rfloor}\right| \underset{n_{2_{\text{opt}}}=\lceil\tilde{n}_2\rceil}{\overset{n_{2_{\text{opt}}}=\lfloor\tilde{n}_2\rfloor}{\lessgtr}} \left|\frac{dT_2}{dn_2}\Big|_{\lceil\tilde{n}_2\rceil}\right|. \tag{20}$$

2) Third Packet: Assuming that the first and second packets propagate at a constant rate of $d_{S_2}^{(2)}$ meters/unit time, the inter-packet separation between the second and third packets just after the third packet is injected is given by $\Delta_3 = n_3 d_{S_2}^{(2)}$, where n_3 is the waiting time of the third packet, as shown in Fig. 7(a). The HQD T_3 for the third packet is: $T_3 = l/d_{S_3}^{(3)} + n_3$. The link condition for the third packet is given as

$$\beta d_{S_3}^{(3)2} + \ln\left[1 + \gamma_t \left/ \left(\frac{n_3 d_{S_2}^{(2)} + \Delta_2^{(3)}}{d_{S_3}^{(3)}} - 1\right)^2\right.\right]$$

$$+ \ln\left[1 + \gamma_t \left/ \left(\frac{n_3 d_{S_2}^{(2)}}{d_{S_3}^{(3)}} - 1\right)^2\right.\right] \leq -\ln(1-\tau). \tag{21}$$
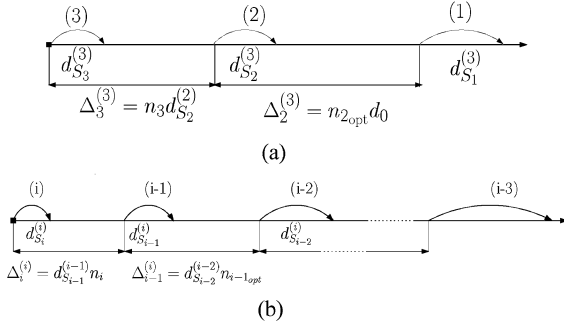
Fig. 7. Recursive optimization of waiting times. (a) Network setting just after the third packet's injection. (b) Network setting just after the ith packet's injection.

To investigate the convexity of T_3 in terms of n_3, it is necessary to study the relationship between $d_{S_3}^{(3)}$ and n_3 under the link condition. We note that the condition can be written as $f_1(d_{S_3}^{(3)}, n_3) + f_2(d_{S_3}^{(3)}, n_3) = c_1 + c_2$, such that $f_1 = c_1$ and $f_2 = c_2$, where c_1 and c_2 are constants. For both functions f_1 and f_2, the waiting time n_3 may be expressed explicitly in terms of $d_{S_3}^{(3)}$. It can be shown that n_3 is convex in $d_{S_3}^{(3)}$ under f_1 and n_3 is linear in $d_{S_3}^{(3)}$ under f_2. A nonnegative weighted sum of two convex functions is also convex [21]. Furthermore, utilizing the fact that $\lim_{n_3 \to \infty} d_{S_3}^{(3)} = d_0$, we conclude that $d_{S_3}^{(3)}$ is concave and is also upper bounded in terms of n_3, i.e., $d_{S_3}^{(3)}(n) < d_0$. Consequently, we may express $d_{S_3}^{(2)} = d_0(1 - e^{-n_3/\alpha_3})$, where α_3 is again a fitting coefficient that is network-dependent. The value of α_3 is greater than that of α_2, since the interference the third packet suffers from at injection is less than that in the case of the second packet. As a result, the optimal waiting time $n_{3_{\text{opt}}}$ for the third packet is obtained by applying the same tools used to derive $n_{2_{\text{opt}}}$.

3) Fourth and Subsequent Packets: Based on the packet decoupling property of Section IV-C4, it is reasonable to assume that the first packet has outpaced the rest of the packets when the fourth packet is to be injected. Therefore, it is sufficient to consider only the second and third packets. The assumption of constant inter-packet separation distances at the vicinity of the source edge still holds. This argument may be generalized for all subsequent packets. Fig. 7(b) depicts the network setting just after the ith packet is injected. The only running variable in this setting is the waiting time n_i of the ith packet. Since only two leading packets are considered, the analysis is identical to the one concerning the injection of the third packet. With the HQD function expressed as

$$T_i = \frac{l}{d_0(1 - e^{-n_i/\alpha_i})} + n_i \tag{22}$$

the optimal waiting time $n_{i_{\text{opt}}}$ is calculated by replacing index 2 in (20) by i.

4) On the Convergence of the Optimal Waiting Time: Here, we provide nontrivial upper and lower bounds for the optimal waiting time and also show that it cannot diverge. We begin by establishing a relationship between the optimal waiting time and the number of leading packets (interferers) as follows.

From Sections V-B2 and V-B3, the noninteger optimal waiting time for packet i is expressed as

$$\tilde{n}_i = \alpha_i \ln \left(\frac{2d_0 \alpha_i}{l + 2d_0 \alpha_i - \sqrt{l^2 + 4ld_0 \alpha_i}} \right) \triangleq \alpha_i \ln \frac{F}{G}.$$

Taking the first derivative of F and G, we obtain $\frac{\partial F}{\partial \alpha_i} = 2d_0$ and $\frac{\partial G}{\partial \alpha_i} = 2d_0(1 - \sqrt{\frac{l}{l + 4d_0 \alpha_i}})$. Since $\frac{\partial F}{\partial \alpha_i} > \frac{\partial G}{\partial \alpha_i}$, $\frac{\partial \tilde{n}_i}{\partial \alpha_i} > 0$ holds. We also have $\frac{\partial d_{S_i}^{(i)}}{\partial \alpha_i} < 0$ and $\frac{\partial d_{S_i}}{\partial \sum_{j=1}^{i-1} d_{I_{ij}}^{(i)}} > 0$. Hence

$$\frac{\partial \tilde{n}_i}{\partial \sum_{j=1}^{i-1} d_{I_{ij}}^{(i)}} > 0 \tag{23}$$

In other words, the optimal waiting time is monotonically increasing in the sum of interference distances. There exists an upper bound on this time based on the following facts.
- The gap between two successive packets features a growing behavior as shown in Section IV-C2.
- For a finite-length network, the number of interferers along a finite linear network is also finite.

Using the result of (23), we are also able to find a lower bound on the optimal waiting time. Since the second packet experiences the least interference, its optimal waiting time $n_{2_{\text{opt}}}$ is the largest and is the lower bound for the optimal waiting times for all packets. On the other hand, if we hypothetically assume that the optimal waiting time diverges, then a direct consequence will be: $\lim_{i \to \infty} \Delta_i^{(i)} = 0$, and $\lim_{i \to \infty} \sum_j d_{I_{ij}}^{(i)} = \infty$. However, this cannot be true based on the fact of finite number of interferers in the network as we have shown above.

For the specific network parameter values of Table I, the optimal waiting time is observed to converge as shown in Fig. 8. This value (denoted by n_w) is mainly affected by the tolerance for outage τ, the SNR, and the network length. The fluctuations that exist in some of the plots of Fig. 8 are due to the fact that the network length is finite. Therefore, the total number of packets might occasionally drop by one, reducing the overall level of interference temporarily. It is clear from Fig. 8 that, the the network conditions are more relaxed, convergence is faster and the optimal value n_w is lower.

5) On the Optimality of the Waiting Time: In optimizing the waiting time, we expressed the HQD in terms of the hopping parameters obtained right after the packet is injected. In Section IV-C, it is shown that, in the long run, the hop distance of a packet increases every new hop. Therefore, it is possible that a packet reaches its destination faster than the calculated HQD. In other words, achieved HQD can be better than the calculated one. For relatively short linear networks, the increase in the hop distance is small such that the actual HQD is not much smaller than the one used in calculating the optimal waiting time.

C. Transport Rate

We will demonstrate now the insufficiency of the transport rate on its own as a metric to characterize the performance of the network. For the ith packet ready to be injected at the head of the source's queue, it was shown in Section V-B3 that HQD and THR are, respectively, expressed as

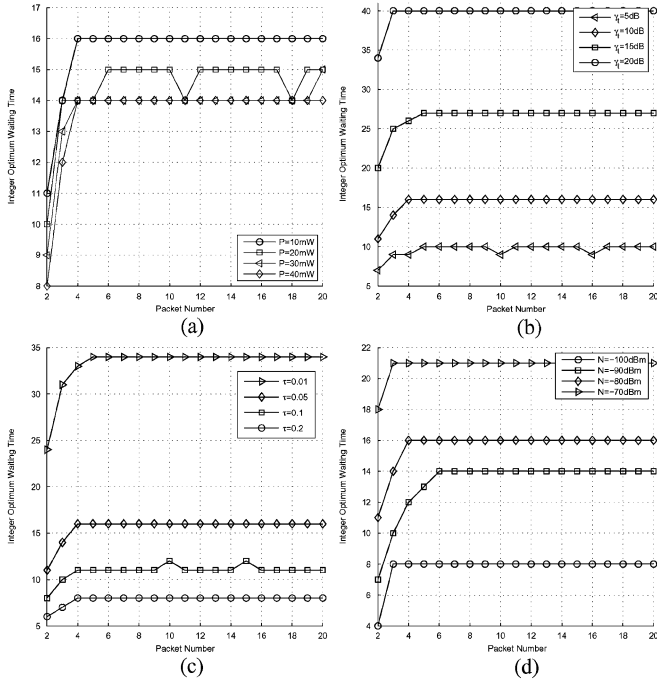$$T_i = \frac{l}{d_0(1 - e^{-n_i/\alpha_w})} + n_i, \quad R = \frac{1}{n_i}. \tag{24}$$

Fig. 8. Convergence of optimal waiting time for different network scenarios. (a) Various transmit powers P. (b) Various SINR thresholds γ_t. (c) Various values of link outage tolerance τ. (d) Various noise powers N.

The transport rate when measured at the source corresponds to the product of the packet injection rate R and the distance a packet covers on its initial hop $d_{S_i}^{(i)}$. Therefore, the transport rate denoted by P, is expressed as

$$P = Rd_{S_i}^{(i)} = \frac{d_0(1 - e^{-n_i/\alpha_i})}{n_i}. \qquad (25)$$

The first derivative of the transport rate in terms of the waiting time n_i is given as

$$\frac{dP}{dn_i} = \frac{d_0}{\alpha_i n_i^2}[e^{-n_i/\alpha_i}(n_i + \alpha_i) - \alpha_i]. \qquad (26)$$

Using the inequality $\ln(\frac{n_i}{\alpha_i} + 1) \leq \frac{n_i}{\alpha_i}$, it can be shown that the transport rate is a monotonously decreasing quantity. However, it was demonstrated in Sections V-B1–V-B3 that HQD is a convex quantity with a global minimum. Consequently, it can be concluded that there must be a compromise in the maximum achievable transport rate if an adequate HQD performance is desired. Since THR is also a monotonously decreasing quantity and is a factor of the transport rate, we chose THR in addition to HQD to jointly reflect the performance of the network.

D. Multi-Objective Optimization in Linear Networks

As discussed in Section V-A, the maximization of source throughput (THR) and the minimization of packet HQD are two conflicting objectives. Thus, their joint optimization has a Pareto optimal solution[1]: the compromise is handled using various approaches, two of which are discussed next.

[1]A feasible point x is Pareto optimal (or efficient) if $f_0(x)$ is a minimal element of the set of achievable values $\mathcal{O}$ [21].

1) Weighted Objectives Method: Objectives are positively weighted and their sum is optimized. Using this method, the problem of finding the optimal waiting time for the ith packet is formulated as follows:

$$\tilde{n}_i = \arg\min_{n_i} w_2\left(\frac{l}{d_0(1 - e^{-n_i/\alpha_i})} + n_i\right) + w_1 n_i \qquad (27)$$

subject to $w_1 + w_2 = 1$ and $w_1, w_2 \geq 0$. The formulation in (27) simplifies to the following:

$$\tilde{n}_i = \arg\min_{n_i} n_i + \frac{w_2 l}{d_0(1 - e^{-n_i/\alpha_i})} \qquad (28)$$

which is the same formulation used previously to minimize the HQD. The only difference here is the factor $0 \leq w_2 \leq 1$ which has the effect of virtually reducing the length of the network. Therefore, the same procedures outlined in Section V-B are used to derive the integer optimal waiting times.

2) Tradeoff Method: The tradeoff method requires the optimization of one objective given the second is bounded. For instance, the problem of maximizing throughput while keeping the HQD below a certain upper bound is formulated as follows:

$$\tilde{n}_i = \arg\max_{n_i} \frac{1}{n_i} \quad \text{s.t.} \quad T_i \leq t_u \text{ and } n_i \geq 2$$

where t_u is some desired upper bound.

VI. OPTIMAL PACKET INJECTION IN MULTIPLE-FLOW MULTIHOP NETWORKS

Here, we consider multiple information sources aligned along one edge and destinations along the opposite edge of a rectangular network. This corresponds to data transfer across a wireless network segment. Throughput (THR) for this scenario is defined as total packet injection rate of M information sources. The definition of HQD is similar to that given for the 1-D case. Our objective in this section is to maximize the total source THR while maintaining HQD for all packets below a certain level. It is shown that this is achieved by:

1) optimally coordinating the packet injection process among information sources;
2) using an optimal combination of the waiting time and the number of flows.

A. Why Parallel and Equally Spaced Flows?

In our analysis, we assume that the number of packet sources equals the number of available packet sinks (destination nodes). We consider equally spaced linear packet flows, i.e., packets progress along parallel linear path trajectories. As a result, packets from one information source are all delivered to the same destination. This combination of parallel and equally spaced flows is selected as it provides minimal inter-flow interference. It was shown in Section III-C that interference experienced by a packet and consequently its hop distance is captured by the sum of interference distances. Given parallel flows, then inter-flow interference is reflected by $\sum_{j=1, j\neq i}^{M} d_{f_{ij}}$, where M is the number of flows and $d_{f_{ij}}$ is the distance between the ith and jth flows. In order to achieve a multiple
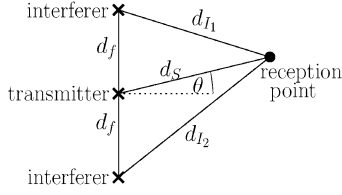
Fig. 9.   Finding point of maximum SIR.

Fig. 10.   Progress of a single synchronous 15-packet wavefront in 20 time units.

parallel flow network with minimal inter-flow interference, we must solve for the set of inter-flow separation distances satisfying M optimization problems. Each of these problems has the following general form:

$$\max \sum_{j=1, j \neq i}^{M} d_{f_{ij}}. \tag{29}$$

A careful inspection will show that these problem have conflicting objectives. A Pareto optimal solution is to have equal inter-flow separation distances.

On the other hand, hopping along equally spaced parallel paths maximizes the SIR. Considering Fig. 9, the SIR at any receiving point in terms of mean signal strengths is given by: $\text{SIR} = \frac{d_S^{-\alpha}}{d_{I_1}^{-\alpha} + d_{I_2}^{-\alpha}}$, where from geometry $d_{I_1}^2 = d_S^2 + d_f^2 - 2d_S d_f \sin \theta$, and $d_{I_2}^2 = d_S^2 + d_f^2 + 2d_S d_f \sin \theta$, i.e., $d_{I_1}^2 + d_{I_2}^2 = 2(d_S^2 + d_f^2)$. For any hop distance d_S, the maximum SIR occurs when $d_{I_1} = d_{I_2}$ at $\theta = 0$. Consequently, it is concluded that the chosen network setting (parallel equidistant flows) provides highly favorable operational conditions.

B. Packet Hopping in Multiple-Flow Networks

The dynamics of packet hopping under intra-flow interference were studied in Section IV. In multiple-flow networks, inter-flow interference must be considered, as well. The effects of inter-flow interference can be understood by considering a network with M sources separated by d_f meters. Let us consider the case where each source injects one packet only, forming a packet wavefront. The progress of a packet towards its destination can be tracked by evaluating the hop distance every time unit. The hop distance of the the ith source's packet at time n is found from the link condition

$$\beta d_{S_i}^2(n) + \sum_{j=1, j \neq i}^{M} \ln\left(1 + \frac{\gamma_t}{\eta_{i,j}(n)}\right) \leq \ln\left(\frac{1}{1-\tau}\right) \tag{30}$$

where

$$\eta_{i,j} = \frac{((i-j)d_f)^2 + (x(j,n) - x(i,n))^2}{d_S^2}$$

such that $x(j,n)$ and $x(i,n)$ are the distances covered till time n by the jth and ith packets respectively. It can numerically be verified that, except for the outermost flows, packets preserve their relative locations as the whole packet wavefront progresses towards the destination edge. This is true regardless of the relative packet injection times. Fig. 10 tracks the progress of the wavefront in time step for arbitrarily selected initial injection locations. This result suggests a trend of uniformity among inner packet flows. In our analysis, we assume that packet flows show
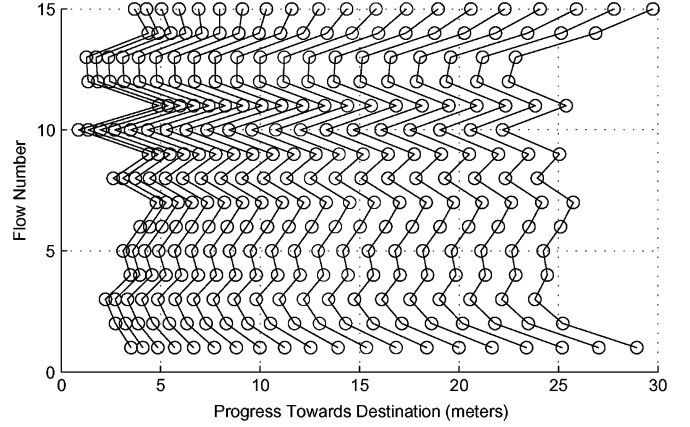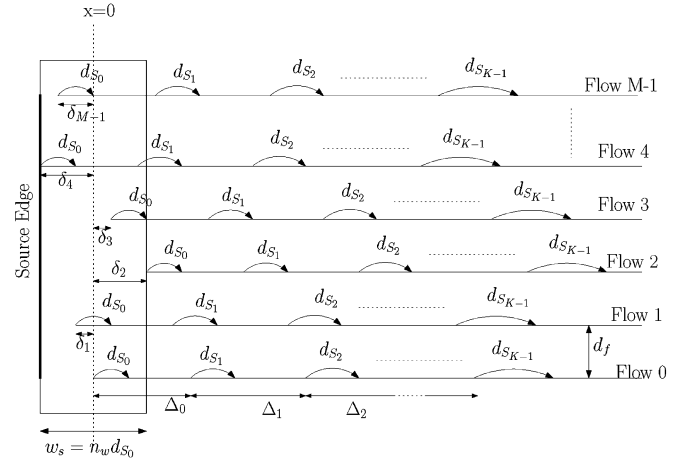

Fig. 11.   Network setting for the multiple-flow problem.

similar hopping behaviors. This assumption is most accurate for flows furthest from network edges.

C. Joint Optimization of THR and HQD in Planar Networks

As in the 1-D case, the network is assumed to have very slow dynamics in the vicinity of the source edge. Identical hopping behavior is assumed for all flows. The error introduced by this assumption is negligible as the number of flows increases. As a result, flows are only shifted versions of each other. The waiting time is the same for all packets injected into the network separated by an offset. For a network with M flows, length l and a waiting time of n_w, THR and HQD are expressed respectively as follows:

$$R_M = \frac{M}{n_w}, \quad T = n_w + \frac{l}{d_{S_0}}. \tag{31}$$

The network setting considered in this problem is shown in Fig. 11. For convenience, packets closest to the source edge are indexed with zero. The problem parameters are given as follows:

- Waiting time: n_w (integer time scale).
- Relative flow displacements: $\underline{\delta} = [\delta_1, \delta_2, \delta_3, \ldots, \delta_{M-1}]$.
- Hopping distances: $\underline{d_S} = [d_{S_0}, d_{S_1}, d_{S_2}, \ldots, d_{S_{K-1}}]$.
- Inter-packet separations: $\underline{\Delta} = [\Delta_0, \Delta_1, \Delta_2, \ldots, \Delta_{K-2}]$.

The *waiting window span* w_s is defined as the maximum distance a packet can hop inside the network before the next packet in the flow is injected, such that $w_s = n_w d_{S_0}$. The set of all optimization parameters is $\underline{v} = [n_w, \underline{\delta}, \underline{d_S}, \underline{\Delta}]$. Under the assumption of uniform flows, $\underline{d_S}$ and $\underline{\Delta}$ are identical for all M flows.

1) Problem Constraints: The joint optimization of THR and HQD in a multiple-flow network is subject to a number of constraints.

- $\Delta_0 = n_w d_{S_0}$, which is also equal to the distance span of the waiting window denoted by w_s.
- $\frac{-w_s}{2} < \{\underline{\delta}\} < \frac{w_s}{2}$. This represents the search span for the relative flow displacements. However, the span actually considered is $[-\frac{w_s}{4}, \frac{w_s}{4}]$ due to the periodical behavior in the other half of the interval.
- $\max \underline{\delta} + \sum_{i=0}^{K-2} \Delta_i \leq l - \frac{w_s}{2}$, i.e., we require that K packets exist in each flow.
- We assume that $d_{S_0} < d_{S_1} < \cdots < d_{S_{K-1}}$ and $\Delta_0 < \Delta_1 < \cdots < \Delta_{K-2}$.
- There are MK link conditions. For the cth packet in the rth flow, the link condition is

$$\beta d_{S_c}{}^2 + \sum_{m=0}^{M-1} \sum_{k=0}^{K-1} \ln\left(1 + \gamma_t \frac{d_{S_c}{}^2}{d_{I_{k,m}}{}^2}\right)$$
$$\leq -\ln(1-\tau) \tag{32}$$
$$d_{I_{k,m}}{}^2 = (r-m)^2 d_f^2$$
$$+ \left[d_{S_c} + \sum_{i=0}^{r-1} \Delta_i - \sum_{j=0}^{k-1} \Delta_j + \delta_r - \delta_m\right]^2.$$

- $d_{S_0} < \Delta_0, d_{S_1} < \Delta_1, \ldots, d_{S_{K-2}} < \Delta_{K-2}$.

2) Testing for Convexity: A convex optimization problem is characterized by having convex objective functions and constraints such that a global optimal is guaranteed. Since for any $\alpha \in \mathbb{R}$ the sublevel sets $M \leq \alpha n_w$ and superlevel sets $M \geq \alpha n_w$ are convex, then R_M is quasi-linear [21]. The THR function belongs to the general class of Quasi-Linear Fractional Functions. On the other hand, the HQD function is convex in terms of n_w and d_{S_0} as it has a positive semidefinite Hessian.[2] As for the link condition, it is not possible to make a judgement about its convexity in its current form. Using $\ln(1+x) \leq x$, (32) can be expressed as $\sum_i (\underline{a}_i^t \cdot \underline{v})^2/(\underline{b}_i^t \cdot \underline{v})^2 + c_i^2$, where $\underline{v}$ is the vector of optimization parameters, $\underline{a}_i$ and $\underline{b}_i$ are parameter selection vectors and c_i is constant. Depending on the values of $\underline{a}_i$, $\underline{b}_i$ and c_i, (32) might be convex, concave, or neither.

3) Approach: Information sources can create a controlled interference environment by controlling the packet waiting times and by coordinating the relative timings of the packet injection. Moreover, the number of flows in a fixed network can be optimally chosen such that optimal network performance is achieved. In other words, we are interested in finding:

1) the optimal mechanism to schedule packet injections into different flows;
2) the optimal number of flows in a network.

A solution for the joint THR-HQD optimization problem can be found by performing a brute force search. This means searching the whole parameters space point by point. However, the di-

mension of the search vector $\underline{v}$ is $M + 2K - 1$. This is large enough to render such an approach very inefficient, especially since some of the search parameters are continuous. However, finding the optimal scheduling pattern and the optimal number of flows does not require a full search. It is actually possible to solve this problem by conducting ad hoc local searches on much smaller subsets of $\underline{v}$, as we will show next.

4) Optimal Schedule: The scheduling problem is completely described by the relative flow displacements $\underline{\delta}$. Moreover, $\underline{\delta}$ does not have an effect on THR. Therefore, the problem of finding an optimal packet injection pattern is addressed by considering the minimization of HQD over $\underline{\delta}$. HQD is minimized when the zeroth wavefront hop distances are maximized for a given waiting window span. This directly corresponds to the minimization of inter-flow interference effects. However, improving one hop distance necessarily deteriorates the others, so we adopt the weighted objectives optimization method. Moreover, we will consider three packet wavefronts. An intra-flow depth of 3 is sufficiently representative of the intra-flow interference effect argued in Section IV-C4. Increasing the depth will only increase the problem's dimension. The problem of finding the scheduling mechanism which optimizes the HQD reduces to

$$\underline{\delta}_{\text{opt}} = \arg\max_{\underline{\delta}} \sum_{m=0}^{M-1} d_{S_0,m} \tag{33}$$

subject to the MK link conditions. The additional subscript m in $d_{S_0,m}$ refers to the flow number. $\underline{\delta}_{\text{opt}}$ is computed by iteratively searching over the relative flow displacements $\underline{\delta}$ while varying the inter-flow separation d_f. The search is done by first discretizing $\underline{\delta} = \{\delta_1, \delta_2, \ldots, \delta_{M-1}\}$ using a low sampling rate. Then, we search over all possible combinations of the discretized $\underline{\delta}$ for the maximum value of $\sum_{m=0}^{M-1} d_{S_0,m}$. For each combination, the value of $\sum_{m=0}^{M-1} d_{S_0,m}$ is found by calculating the individual hop distances $\{d_{S_0,m}\}_{m=0}^{m=M}$ using (32). The relative flow displacements that have yielded the maximum value are recorded. In the next iteration, we increase the rate at which $\underline{\delta}$ is sampled. The search for a maximum is done again. The search range is reduced to include only the vicinity of the optimal relative displacements from the previous iteration. This continues until the change in the calculated maximum from one iteration to the next falls within a certain range. Numerical results show that the optimal relative flow displacements occur when flows are alternately shifted half-way the waiting window span as shown in Fig. 12. This is true for inter-flow separations as small as 10% of the waiting window span. We conclude that sources must alternately schedule their packet injections so that the shown HQD-minimizing pattern is attained. For smaller values of d_f, the optimal relative displacements feature larger disparity to accommodate the vanishing inter-flow separation distance of successive flows.

5) Optimal Number of Flows: Under a tradeoff approach, we wish to maximize THR subject to HQD $\leq t_u$, where t_u is a desired delay upper bound. We also use here three packet wavefronts, i.e., $K = 3$. We take $\Delta_1 \approx \Delta_0$ for simplicity. This will impose only a marginal amount of error but will largely reduce the computational burden. Moreover, the optimal scheduling pattern found in Section VI-C4 is used. Under the assumption of slow hopping dynamics, d_{S_0} is approximately constant

---

[2]A function f with a positive semidefinite Hessian has $\Delta^2 f(x) \succeq 0$ [21].
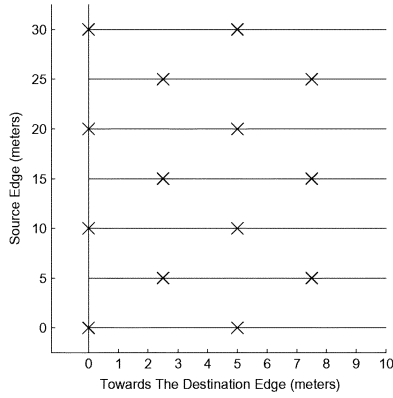
Fig. 12.   Optimal packet transmitter pattern for $M = 7$ flows and $d_f \geq 0.1w_s$.

inside the waiting window w_s. Therefore, THR and HQD are evaluated respectively as

$$R_M = \frac{Md_{S_0}}{w_s}, \quad T = \frac{(l + w_s)}{d_{S_0}}. \tag{34}$$

There are three control variables in (34): w_s, M, and d_{S_0}. However, if w_s and M are given, all hop distances including d_{S_0} can be found from the link conditions in (32). In order to find the optimal combination of w_s and M, their values are varied and the corresponding HQD and THR are evaluated. This is done by first evaluating the hop distances in (32).

We perform calculation for a sample network of 500×500 m. The results are presented in terms of the contour and surface plots shown in Fig. 13. Under the tradeoff optimization approach, there exists a set of optimal operating points which depend on the upper bound t_u. For a certain value of t_u, the maximum achievable THR is given by the R_M contour level, which is tangent to the contour level $T = t_u$. The optimal number of flows and waiting window span are given by the tangency point. Hence, M_{opt} and $w_{s_{\text{opt}}}$ are found by solving the equation $\nabla R_M = \nabla T$.

D. Numerical Examples

Assuming 100-byte long packets and a data rate of 1 Mbps, one time unit is 0.8 ms. The transmit power is 10 dBm. In the first example, we consider $t_u = 250$ time units. The maximum network THR corresponding to this value may be numerically found by sweeping through the level contours of R_M in the ascending direction of its gradient until the tangency point is reached. This is shown in Fig. 14(a). A maximum THR of 231 kbps is achieved. The optimal parameters are $w_{s_{\text{opt}}} = 53.5$ m and $M_{\text{opt}} = 5.58$. However, the actual operational point is $M = \lfloor 5.58 \rfloor = 5$ flows and $w_s = 48.0$ m. This keeps the HQD at the maximum level of 250 but reduces the achievable throughput to slightly below 231 kbps. The optimal inter-flow separation is $d_f = 125$ m and the corresponding initial packet hop distance is 2.192 m. As a result, the optimal integer waiting time equals 22 time units (17.6 ms). In other words, a packet must wait 17.6 ms at the head of the source queue before being injected. The transfer delay to the destination is at most 200 ms.

Another illustrative example is the 1-THR case, i.e., THR $= 1$ Mbps. As shown in Fig. 14(b), we fix the contour level corresponding to $R_M = 1$ packet/unit time, and we
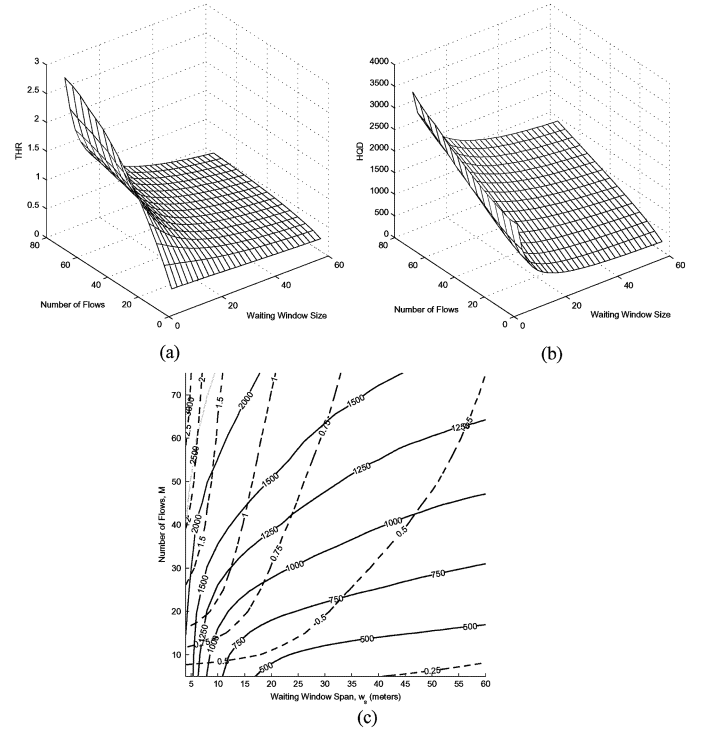

Fig. 13.   Surface and contour plots for the multiple flow optimization problem. (a) THR versus window size w_s and number of flows M. (b) HOD versus window size w_s and number of flows M. (c) Level contours: THR (dashed line) and HQD (solid line).
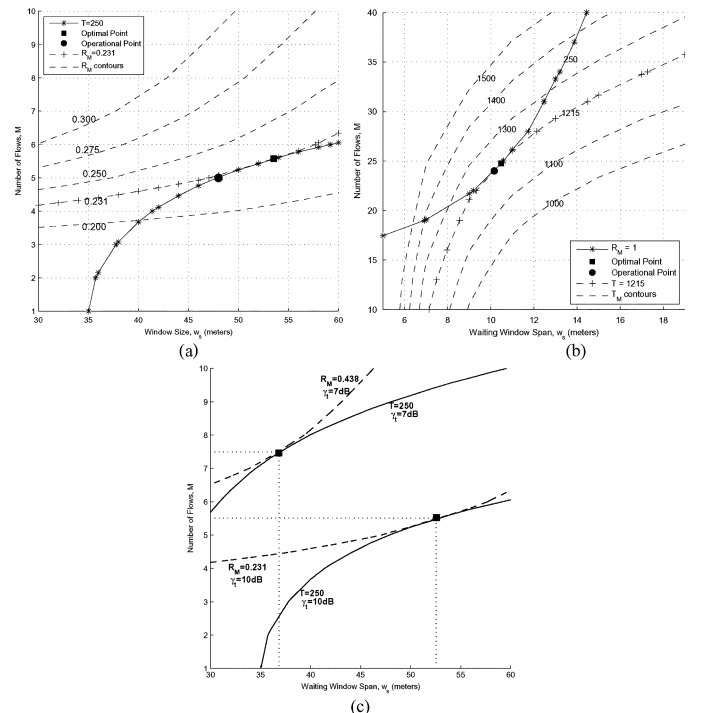

Fig. 14.   Multiple-flow optimization examples with tradeoff approach. (a) Example 1: Max THR for $\text{HQD} \leq 250$. (b) Example 2: 1-THR case. (c) Effect of SINR threshold γ_t on Performance.

sweep through contours of the HQD function until the tangency point is reached, which happens to lie on the HQD contour curve $T = 1215$ time units (972 ms). The optimal point is $w_{s_{\text{opt}}} = 10.48$ m and $M_{\text{opt}} = 24.77$. The actual operating

TABLE III
TWO EXAMPLES UNDER TRADEOFF OPTIMIZATION METHOD

	Max THR for HQD$\leq$ 250	Unit-THR
THR, R_M	231 Kbps	1 Mbps
HQD, T	0.200 s	0.972 s
Waiting Window Span, w_s	48.0 m	10.16 m
Number of Flows, M	5 flows	24 flows
Inter-Flow Separation, $d_{f_{opt}}$	125 m	21.74 m
Initial Hop Distance, d_{S_0}	2.192 m	42 cm
Optimal Waiting Time, $n_{w_{opt}}$	17.6 ms	20.0 ms

TABLE IV
COMPARISON OF MAXIMUM ACHIEVABLE THR UNDER DIFFERENT SINR
THRESHOLDS, WITH HQD $\leq$ 250

γ_t	7dB	10dB
max R_M	438Kbps	231Kbps
$d_{f_{opt}}$	83.3m	125m
d_{S_0}	2.137m	2.192m

point is $M = \lfloor 24.77 \rfloor = 24$ flows and $w_s = 10.16$ m which lies on the $T = 1215$ contour level and gives a THR almost equal to 1 Mbps. This corresponds to an optimal inter-flow separation of 21.74 m, an initial packet hop distance of 42 cm and an optimal waiting time of 25 time units. The results of both examples are summarized in Table III.

The above two examples strongly convey the shortcoming of considering the transport rate as the *only* performance metric. This is illustrated by considering the transport rates obtained for the networks in both examples. In the first example, the transport rate is 506 kb·m/s and in the second example it is 420 kb·m/s. While the transport rates in both cases are comparable, the high contrast in the values of THR and HQD is evident. The HQD and THR in the second example are almost five times those in the first. Apparently, the transport rate does not fully capture the actual behavior of the network. Therefore, judging the network performance solely based on the transport rate is insufficient.

It is also interesting to investigate the effect of the SINR decodability threshold γ_t on the performance of the multihop network. The results of the first example in Section VI-D were evaluated using $\gamma_t = 10$ dB. Assuming that a better decoding scheme is able to provide a 3 dB decoding gain, i.e., γ_t can be lowered to 7 dB, then we expect to similarly obtain a gain in performance. To verify this, we fixed the maximum allowable HQD at $T = 250$, and reran the calculations performed for the first example in Section VI-D but with $\gamma_t = 7$ dB. The results are shown in Fig. 14(c). As expected, the maximum achievable throughput for the case of $\gamma_t = 7$dB was improved. THR increased by almost a factor of 2 as shown in Fig. 14(c). Results also show that the decreased decodability threshold allows for a larger number of flows to be packed in the network, hence improving THR. On the other hand, this also comes at the expense of the node density required to maintain the desired performance in the mean sense. It can be shown that the grid size in the case $\gamma_t = 7$ dB is approximately 1.54 times that when $\gamma_t = 10$ dB. The results of this example are summarized in Table IV.

VII. CONCLUSION

In this paper, we analyze packet streaming in interference-limited multihop networks. We consider throughput (THR) and head-of-queue delay (HQD) as performance criteria. We express both criteria in terms of the packet flows rather than the individual packet transmissions. The analysis is carried out for a Rayleigh fading environment. It is shown that the probabilistic link model given in [7] is suitable to use in block fading (quasistatic) as well as fast (time-selective) fading scenarios. A communication model is built accordingly and used to develop a framework of packet hopping models.

The optimal network performance is achieved in a controlled environment. The packet injection process is subject to temporal and spatial constraints such that the desired performance balance is obtained. It is shown that waiting times must be introduced between the injections of subsequent packets. For a fixed-size network, the number of flows must also be considered in the optimization problem. In the 1-D case, recursive optimization is performed and the optimal waiting time is derived. In the 2-D case, it is shown that the total search space may be reduced into smaller subspaces. This is achieved by decoupling the effects of optimization parameters and solving sub-problems sequentially. With this approach, we have investigated the achievable performance bounds in THR (HQD), when HQD (THR) is used as a performance constraint.

In our future work, we will consider random node positions in finite-density networks. We will treat packet flows as vector quantities, and develop the analysis accordingly. Moreover, we will consider non-integer continuous time steps, where packet transmissions need not be synchronized. We will then consider the relationship between routing strategies and inter-flow interference.

REFERENCES

[1] P. Gupta and P. R. Kumar, "The capacity of wireless networks," *IEEE Trans. Inf. Theory*, vol. 46, no. 2, pp. 388–404, Mar. 2000.

[2] A. Agarwal and P. R. Kumar, "Capacity bounds for ad hoc and hybrid wireless networks," *ACM SIGCOMM Comput. Commun. Rev.*, vol. 34, no. 3, pp. 71–81, Jul. 2004.

[3] F. Xue, L.-L. Xie, and P. R. Kumar, "The transport capacity of wireless networks over fading channels," *IEEE Trans. Inf. Theory*, vol. 51, no. 3, pp. 834–847, Mar. 2005.

[4] S. Toumpis, "Capacity bounds for three classes of wireless networks: Asymmetric, cluster, and hybrid," in *Proc. 5th ACM Int. Symp. Mobile Ad Hoc Netw. Comput.*, 2004, pp. 133–144.

[5] G. Barrenechea, B. Beferull-Lozano, and M. Vetterli, "Lattice sensor networks: Capacity limits, optimal routing and robustness to failures," in *Proc. 3rd Int. Symp. Inf. Process. Sensor Netw.*, Apr. 2004, pp. 186–195.

[6] E. S. Sousa and J. A. Silvester, "Optimum transmission ranges in a direct-sequence spread-spectrum multihop packet radio network," *IEEE J. Sel. Areas Commun.*, vol. 8, no. 5, pp. 762–771, Jun. 1990.

[7] M. Haenggi, "Toward a circuit theory for sensor networks with fading channels," in *Proc. Int. Symp. Circuits Syst.*, May 2004, vol. 4, no. IV, pp. 908–911.

[8] K. Jain, J. Padhye, V. Padmanabhan, and L. Qiu, "Impact of interference on multi-hop wireless network performance," in *Proc. ACM MobiCom*, San Diego, CA, 2003, pp. 66–80.

[9] R. Hekmat and P. Mieghem, "Study of connectivity in wireless ad hoc networks with an improved radio model," in *Proc. 2nd Workshop Model. Optim. Mobile, Ad Hoc, Wireless Netw.*, Mar. 2004, pp. 142–151.

[10] R. Hekmat and P. Mieghem, "Interference in wireless multi-hop ad hoc networks and its effect on network capacity," *Wireless Netw.*, vol. 10, no. 4, pp. 389–399, Jul. 2004.

[11] J. Gronkvist, "Traffic controlled spatial reuse TDMA in multi-hop radio networks," in *Proc. 9th IEEE Int. Symp. Pers., Indoor Mobile Radio Commun.*, Sep. 1998, vol. 3, pp. 1203–1207.

[12] T. S. Rappaport, *Wireless Communications: Priciples and Practice*, 2nd ed. Upper Saddle River, NJ: Prentice-Hall, 2001.

[13] M. Simon and M. S. Alouini, *Digital Communication over Fading Channels*, 2nd ed. New York: Wiley, 2005.

[14] M. Haenggi, "Probabilistic analysis of a simple MAC scheme for ad hoc wireless networks," in *Proc. IEEE CAS Workshop Wireless Commun. Netw.*, 2002.

[15] M. Haenggi, "On routing in random Rayleigh fading networks," *IEEE Trans. Wireless Commun.*, vol. 4, no. 7, pp. 1553–1562, Jul. 2005.

[16] M. Haenggi, "Analysis and design of diversity schemes for ad hoc wireless networks," *IEEE J. Sel. Areas Commun.*, vol. 23, no. 1, pp. 19–27, Jan. 2005.

[17] J. Lai and N. B. Mandayam, "Minimum duration outages in Rayleigh fading channels," in *Proc. 31st Ann. Conf. Inf. Sci. Syst.*, 1997.

[18] N. B. Mandayam, P.-C. Chen, and J. M. Holtzman, "Minimum duration outage for cellular systems: A level crossing analysis," in *Proc. IEEE Veh. Technol. Conf.*, 1996, vol. 2, pp. 879–883.

[19] A. Ephremides, "Energy concerns in wireless networks," *IEEE Wireless Commun.*, vol. 9, no. 4, pp. 48–59, Aug. 2002.

[20] L. Sankaranarayanan, G. Kramer, and N. B. Mandayam, "Hierarchical sensor networks: Capacity bounds and cooperative strategies using the multiple-access relay channel model," in *1st Ann. IEEE Commun. Soc. Conf. Sensor and Ad Hoc Commun. Netw.*, Oct. 2004, pp. 191–199.

[21] S. Boyd and L. Vandenberghe, *Convex Optimization*. Cambridge, U.K.: Cambridge Univ. Press, 2004.

Ahmed Bader received the B.S. degree in electrical engineering (with highest honors) from the University of Jordan, Amman, Jordan, in 2003, and the M.S. degree in electrical and computer engineering from The Ohio State University, Columbus, in 2006.

He is currently a Senior Wireless Engineer with VTEL Holdings, Amman. His research interests include wireless multihop and mesh networks focusing on channel modeling and interference management.

Eylem Ekici (S'99–M'02) received the B.S. and M.S. degrees in computer engineering from Boĝaziçi University, Istanbul, Turkey, in 1997 and 1998, respectively, and the Ph.D. degree in electrical and computer engineering from the Georgia Institute of Technology, Atlanta, in 2002.

Currently, he is an Assistant Professor with the Department of Electrical and Computer Engineering, Ohio State University, Columbus. His current research interests include wireless sensor networks, vehicular communication systems, next generation wireless systems, and space-based networks, with a focus on routing and medium access control protocols, resource management, and analysis of network architectures and protocols. He is an Associate Editor of *Computer Networks Journal* and *ACM Mobile Computing and Communications Review*. He also served as the TPC co-chair of the IFIP/TC6 Networking 2007 Conference. He has been a member of the ACM since 1999.